

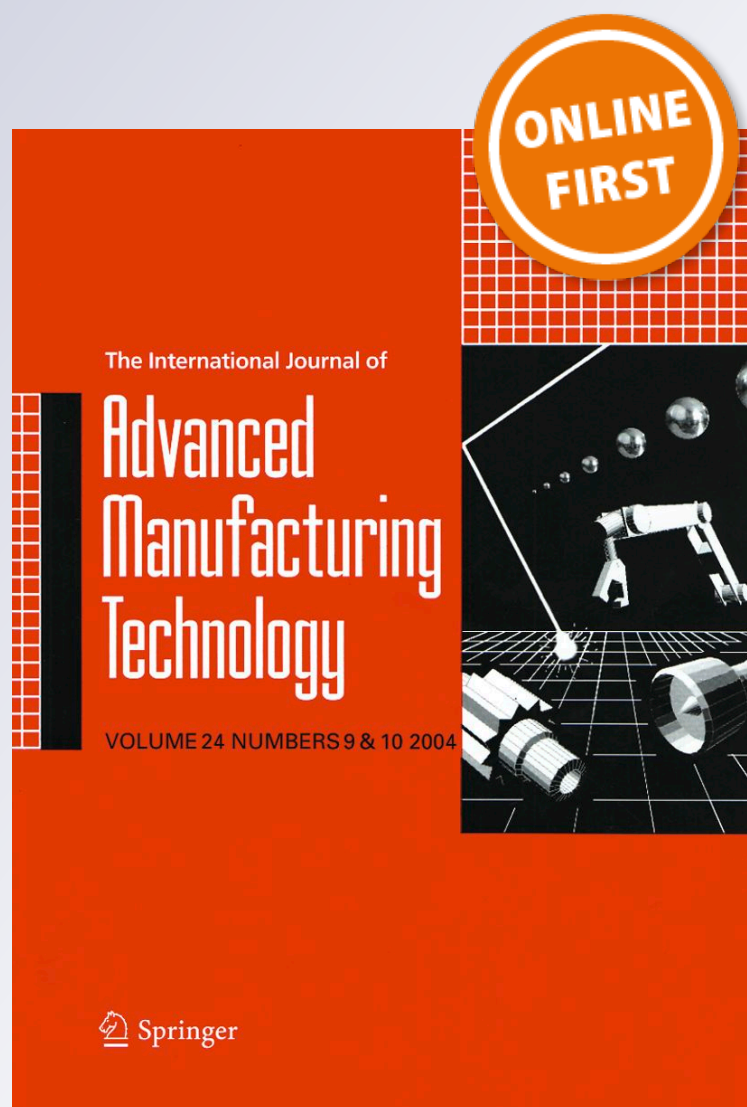
Friction capabilities of graphite-based lubricants at room and over 1400 K temperatures

**A. J. Sánchez Egea, V. Martynenko,
G. Abate, N. Deferrari, D. Martinez
Krahmer & L. N. López de Lacalle**

**The International Journal of
Advanced Manufacturing Technology**

ISSN 0268-3768

Int J Adv Manuf Technol
DOI 10.1007/s00170-019-03290-4



Your article is protected by copyright and all rights are held exclusively by Springer-Verlag London Ltd., part of Springer Nature. This e-offprint is for personal use only and shall not be self-archived in electronic repositories. If you wish to self-archive your article, please use the accepted manuscript version for posting on your own website. You may further deposit the accepted manuscript version in any repository, provided it is only made publicly available 12 months after official publication or later and provided acknowledgement is given to the original source of publication and a link is inserted to the published article on Springer's website. The link must be accompanied by the following text: "The final publication is available at link.springer.com".



Friction capabilities of graphite-based lubricants at room and over 1400 K temperatures

A. J. Sánchez Egea^{1,2} · V. Martynenko^{3,4} · G. Abate^{3,4} · N. Deferrari³ · D. Martinez Krahmer^{3,4} · L. N. López de Lacalle²

Received: 25 September 2018 / Accepted: 2 January 2019
© Springer-Verlag London Ltd., part of Springer Nature 2019

Abstract

The present work investigates the lubricant capabilities at room and hot-forging temperatures (>1400 K) of three types of lubricants with two different graphite concentrations (8% and 12%). These lubricants are distinguished by measuring the percentage of chemical elements and average size of graphite particles. Later, two standardized methods, i.e., pin-on disc and ring test, are utilized to assess the main friction differences under laboratory and real industry conditions, respectively. The results exhibit that the friction values at room temperature are lower for lubricant B, no matter which type of graphite concentration is used, whereas at hot-forging temperatures, greater percentage of graphite enhances lower frictional values when higher deformations are assessed. Additionally, the ring tests performed at hot-forging temperatures show significant tribology differences when the degree of deformation reaches 50%. Particularly, the lubricant B shows the lowest values of friction coefficients of 0.22 and 0.21 for 8% and 12% of graphite concentration, respectively. Therefore, it can be concluded that the selection of a proper type of lubricant (regarding chemical composition and size of solid suspension) and the graphite concentration are sensitive parameters, when it comes to achieve different bulk deformations combined with extreme temperatures like in hot-forging process.

Keywords Graphitic lubricant · Extreme temperatures · Friction coefficients · Ring test · Hot-forging

1 Introduction

Lubricant properties such as viscosity, stability, and lubricity are temperature dependent, which are closely related to friction, durability, and efficiency. Two techniques are commonly used to assess the lubricant properties, i.e., the pin-on disc to determine the friction coefficients and wear rate and the ring test to analyze the behavior of lubricants used in plastic forming processes [1]. The ring test can be performed at

different temperatures which allows studying the lubricant behavior in real industry scenarios such as cold, warm, and hot forging. The tribological analysis of lubricants with the aforementioned tests is widely investigated to determine the friction coefficients, where several aspects provide particular relevance: the influence of operational parameters, environmental conditions (temperature, pressure, chemical components...), and type of materials combined with the geometrical configurations of interfaces to interact.

✉ A. J. Sánchez Egea
antonio.egea@ing.puc.cl; antonio.egea@ehu.eus

V. Martynenko
vmart@inti.gob.ar

G. Abate
gabate@inti.gob.ar

N. Deferrari
deferrari@inti.gob.ar

D. Martinez Krahmer
mkrahmer@inti.gob.ar

L. N. López de Lacalle
norberto.lzlacalle@ehu.eus

¹ Department of Mechanical and Metallurgical Engineering, Pontificia Universidad Católica de Chile, Av. Vicuña Mackenna 4860, 7820436 Santiago, Región Metropolitana, Chile

² Department of Mechanical Engineering, Faculty of Engineering of Bilbao, Aeronautics Advanced Manufacturing Center (CFAA), Alameda de Urquijo s/n, 48013 Bilbao, Spain

³ Centro de Investigación y Desarrollo en Mecánica, Instituto Nacional de Tecnología Industrial INTI, Avenida General Paz 5445, 1650 Miguelete, San Martín, Provincia de Buenos Aires, Argentina

⁴ Faculty of Engineering, Universidad Nacional de Lomas de Zamora, Juan XXIII y Camino de Cintura, Lomas de Zamora, Provincia de Buenos Aires, Argentina

At first, the influence of operational parameters can be observed in a large number of experimental studies, for instance, the relationship between the deformation rate and the degree of barreling was observed while studying the friction behavior. Accordingly, four types of curves were found which strictly depend on the two mentioned parameters [2]. Similar results were found by Camacho et al. [3] who also introduced the influence of different metallic alloys. González et al. [4] predicted the material texture removal of different metallic alloys based on the previous milling surface characteristics. The wear coefficient took into account the influence of speed on the abrasive material, the applied force, type of material, and the size of abrasive grains to describe the abrasive mechanism. As a result, they exhibited linear trend between the sizes of abrasive grain for each metallic alloy. Additionally, the speed of application of the load was studied to compare incremental forces (hammer upsetting) or continuous forces (mechanical press upsetting) [5]. Experimental and numerical approximations were found in the case of metal forming under heavy regimes for low compression ($< 20\%$) scenarios. Consequently, Camacho et al. [6] reported the possibility of considering a single friction coefficient. The friction results will vary due to the compression values, where an average value should be considered to estimate the friction coefficient from the steps of different forces. Furthermore, the surface roughness between the interfaces is a sensitive parameter to take into account. Some experiments performed with the ring test showed that the rings with texture of higher surface roughness bring higher friction values [7]. Moreover, the same experiments were performed in aluminum AA6061 T6 by combining two types of lubricants, three forge temperatures, three deformation speeds, and three degrees of deformation. As a result, it was observed that one of the lubricants displayed a constant response independent of the conditions, as described by Oliveira et al. [8]. Therefore, the type of lubricant is crucial to reduce the friction coefficient during hot-forging temperatures.

On the other hand, the type of material and the geometrical configurations of the interfaces to interact have been well investigated to assess the friction for each case. Hence, the friction tests have been carried out in modern materials, such as Ti6Al4V alloy [9], micro-alloyed steel with half carbon [10], and Nimonic 115 [11]. Regarding the geometrical design, the dispersions of the coefficient of friction were commonly found during the ring test which derive from the irregular shape of the inner diameter of the deformed ring. Hu et al. [12, 13] proposed to add a thin wing at half of its thickness to measure the material's deformation. This element is not in contact with the plates, and subsequently, a lower geometrical distortion degree is expected. However, although the roundness of diameter of the wing was maintained, all the samples tested showed different degrees of warping, which complicate the measurements. The same experiments were conducted by

changing the design of the wing to overcome the aforementioned difficulties. Later, Sánchez et al. [14] proposed an easy and affordable methodology to estimate the forging capacity of a mechanical press. The numerical simulation was used to calculate the bulk deformation of metallic alloy in a single stroke, which can help to investigate the efficiency of the lubricants at different compression values.

Moreover, the environmental conditions at the contact surfaces will have a relevant importance in the tribology analysis. So, the oxide film resulting from hot forging should be considered in the friction scenarios, as well as the surface roughness and the contact areas. Cristino et al. [15, 16] found that the oxidation increased the friction by 30%, whereas the friction curve versus the surface roughness exhibited a sigmoidal adjustment. Moreover, Matsumoto et al. [17] did not find any friction enhancement when the oxide layer formed due to water vapor in the interface of chromium steels. Despite the layer is being porous and has low thermal conductivity, these characteristics did not contribute to reduce friction. Temperature is another important parameter to take into account in relation to the friction coefficients. Zhu et al. [18] analyzed the friction curves and the variation of internal diameters of the tested rings which depend on the heat transfer coefficient. A review about the tribological effects in metal forming at elevated temperature defined four aspects to take into account the interaction between tool and specimen: oxidation, coating, lubricant, and tribometers [19]. Considering the lubricant effects in tribology, Li et al. [20] described the tribological effects of graphitic lubricants on Ti6Al4V alloy for temperature above 1000 K. They found that the graphitic lubricants reduced the friction coefficient during the ring test, although the friction coefficient was strictly dependent of the temperature. At higher temperatures, the lubricant became less effective since greater friction coefficient values were witnessed. Additionally, Asai et al. [21, 22] evaluated the behavior of several types of lubricants by using thermogravimetric techniques. They found that non-graphite lubricants evaporated completely before reaching 700 K, while the graphitized lubricants could achieve temperatures within the range of 1000 to 1500 K and the 40% amount of the lubricant remained active in view of the tested configuration at room temperature.

Following the aforementioned research topics, the present work focuses on studying the friction behavior of three different graphitic lubricants with two concentrations of graphite (8% and 12%) for room and 1400 K temperatures. Initially, the three lubricants are characterized to define their chemical composition and the size of graphite embedded in the matrix. Then, the pin-on disc and ring test are carried out to determine the friction coefficients depending on the type of lubricant, graphitic concentration, bulk deformation, and temperature. Therefore, the proper lubricant characteristics and operational forming parameters can be recommended to perform an

efficient hot-forging process, where extreme temperatures complicated the use of other types of lubricants.

2 Methodology

The methodology of this work is divided into three subsections: characteristics of lubricants, pin-on disc test at room temperature, and ring test at hot-forging temperatures. Consequently, along these subsections, the protocols, devices, and facilities utilized to investigate the lubricant efficiency at different temperatures and bulk deformations are explained.

2.1 Characteristics of lubricants

Three different lubricants were used in the present work: lubricant A, lubricant B, and lubricant C with two different graphite concentrations, i.e., 8% and 12%, which are the graphite concentrations used by CRAFTSA in the small- and medium-sized forging components, respectively. The three lubricants had 22% of solid suspension in water as a dilute and the density about 1.10 and 1.20 g/cm³. In order to characterize and describe the main differences amongst the three lubricants, a scanning electron microscope (FEI model: QUANTA 250 FEG) was utilized to measure the particle size embedded in the matrix for each lubricant. Additionally, a scanning electron microscope (model: Philips SEM 505) equipped with the energy-dispersive x-ray spectroscopy module (UTW-Sapphire, model: PV7760/79 ME) was deployed to study the chemical composition of the three graphite-based lubricants. In particular, a standardless quantification analysis was considered for the quantitative results of x-ray spectra.

2.2 Pin-on disc test at room temperature

The pin-on disc tests were carried out with an in-house machine at the INTI-Mechanics Center in Argentina. The procedure to do the pin-on disc was the following: firstly, the 20 tips of the pins made of SAE 1045 carbon steel (with a Φ 6 mm stem and spherical tip of Φ 4 mm in both ends) were polished with abrasive papers of grain sizes 100, 600, and 1000. At the same time, 20 discs of SAE H13 tool steel (external diameter of Φ 63 mm, internal diameter of Φ 19 mm, and thickness of 6 mm) were grinded by a tangential grinding machine (the same one used in Sánchez et al. [23]) with a grinding wheel (model: A46H10V). The force during the pin-on disc test was recorded with a data logger (Vernier model LabQuest) and a load range of 50 N. The surface roughness of the specimens was measured with a portable profilometer (model: Taylor Hobson Surtronic 3+). Table 1 shows the average surface roughness of the specimens used in the pin-on discs' experiments, where the cutoff and the evaluation length were set in 0.8 mm and 4 mm, respectively.

Table 1 Surface roughness of the specimens tested in the pin-on disc

Parameter	Av. surface roughness parallel to the grinding direction	Av. surface roughness perpendicular to the grinding direction
Ra (μ m)	0.34	0.68
Rt (μ m)	2.70	5.50

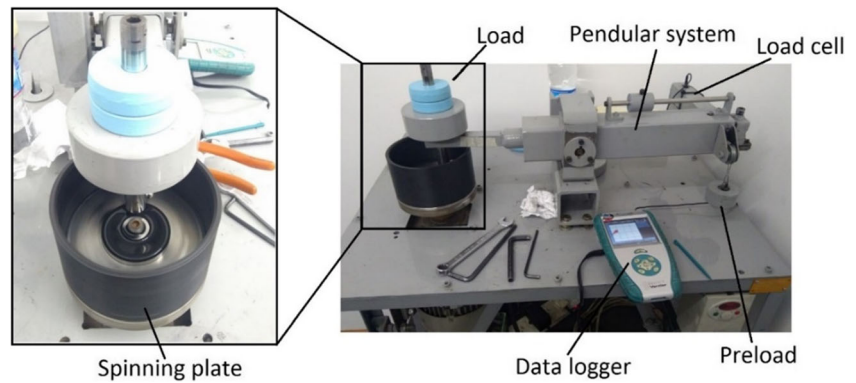
Later, the disc and the pins were allocated in the pin-on discs' machine to perform the experiment. Subsequently, the graphite-based lubricant was added on the disc and verified the proper dispersion of the lubricant all over the specimen before running the test. The applied load of the tip on the disc was set at 6.5 N; the tangential velocity was 0.2 m/s at the contact area of the tip and disc. The ring test took 20 min and the friction values were found to be stable after 10 min. Finally, these experiments were repeated 36 times with the combination of three types of graphitic lubricants, two graphite concentrations, and six repetitions per combination. Figure 1 shows the pin-on disc test carried out by in-house tribometer manufactured at the INTI-Mechanics Center in Argentina.

2.3 Ring test at hot-forging temperatures

In total, 24 rings made of SAE 1045 carbon steel specimens previously round turned were used in the ring tests. These experiments were carried out at the workshop of CRAFTSA S.A. in Argentina. The compression tests were assessed with a universal mechanical press of 1300 t (model: AJAX National Maxipress), and the upsetting velocity of the hammer was 0.2 m/s. Accordingly, Table 2 shows the initial configuration of the tested specimens in the ring test.

To estimate the forging loads during the ring test under different degrees of deformations and friction coefficients, several numerical simulations were carried out to study the compression behavior, similar to the method explained in Sánchez et al. [14]. A continuous horizontal induction furnace (model: Newelco 400 kW) was used to achieve temperatures of 1400 K. The geometrical dimensions were measured with a digital caliper (model: Tesa 8H242906), whereas the temperature was recorded with an IR camera (model: Minolta Lands Cyclops 153) with an accuracy of $\pm 0.5\%$. The surface roughness of the specimens was measured with the same profilometer. During the ring test, a total of 24 assays were carried out with the combination of three types of graphitic lubricants, two graphite concentrations, and four degrees of deformation. Figure 2 shows the ring test carried out with the hot forging press at the CRAFTSA S.A. workshop of Argentina.

Fig. 1 Description of the main components of the in-house tribometer used to perform the pin-on disc test at room temperature



3 Results

The results of the present work are divided in three subsections. Firstly, the properties and the intrinsic characteristics of each lubricant are described with the purpose of comparing and highlighting the differences amongst them. Then, the friction coefficient at room temperature is studied with the pin-on disc test, and ultimately, the tribology behavior of each lubricant is investigated during ring test at high temperatures (hot-forging process).

3.1 Lubricant properties and characteristics

The type lubricant and graphite concentration described the main tribological differences in the present study, so it is necessary to characterize each type of lubricant. Figure 3 highlights the size of the graphite embedded in the matrix of each graphite-based lubricant, whereas Table 3 quantifies the average grain size and the percentage weight of chemical composition.

The results indicate that the grain size of the graphite embedded in the matrix of the lubricant B is 4.5 and 4.0 times smaller in average than the graphite size of lubricants A and C, respectively. The margin errors represent the standard deviation of ten measurements per each lubricant, which shows the large variability of the grain size of the graphite embedded in the matrix. The graphite size can enhance the tribological capabilities, as described by Gunda and Narala [24] while studying the effectiveness of the particle size of solid lubricants under extreme temperatures, loads, and speeds. Additionally, lubricant B exhibits higher percentage weight of silicon and aluminum, which can promote a larger formation of silicate

compounds and alumina. These compounds have been proven to reduce the friction coefficient and wear characteristics up to 46%, as stated by Devendra et al. [25] during a four-ball tribometer experiment. Accordingly, the following sections focused to investigate the friction coefficients at room temperature using pin-on disc and at high temperatures by using ring test to describe the characteristics of tribological capabilities of these graphitic lubricants.

3.2 Friction coefficients at room temperature

The friction coefficient at room temperature has been analyzed by using the pin-on disc test. The behavior of the lubricant is assessed in a period of 20 min, in order to ensure a stable contact between the pin and sample's surface and, consequently, determine the friction coefficient. Figure 4 exhibits the friction behavior at room temperature of the three lubricants over time for the two types of graphite concentrations.

At the beginning of the test, the friction coefficient tends to increase in all the cases; then, a constant friction behavior is reached when the lubricant is homogeneously distributed over the specimen surface and a stable contact between the pin and specimen's surface is achieved. However, a dispersion error of the friction coefficient in each lubricant is observed, which derived from the surface irregularities of each specimen. In both graphite concentrations, the lubricant B presents lower values of friction coefficients with respect to the other two configurations, emphasizing the concentration of graphite of 8%. Figure 5 presents a boxplot to statistically compare the friction results found at room temperature. In this way, the average and error dispersions can be determined to define the differences amongst the lubricants and their graphite

Table 2 Initial geometrical parameters of the specimen used in the ring test

Parameter	Height (mm)	Ext. diam. (mm)	Int. diam. (mm)	Inf. Ra (μm)	Sup. Ra (μm)
Average	18.274	55.054	27.521	2.720	3.257
Error (ST)	0.058	0.216	0.120	0.690	0.491

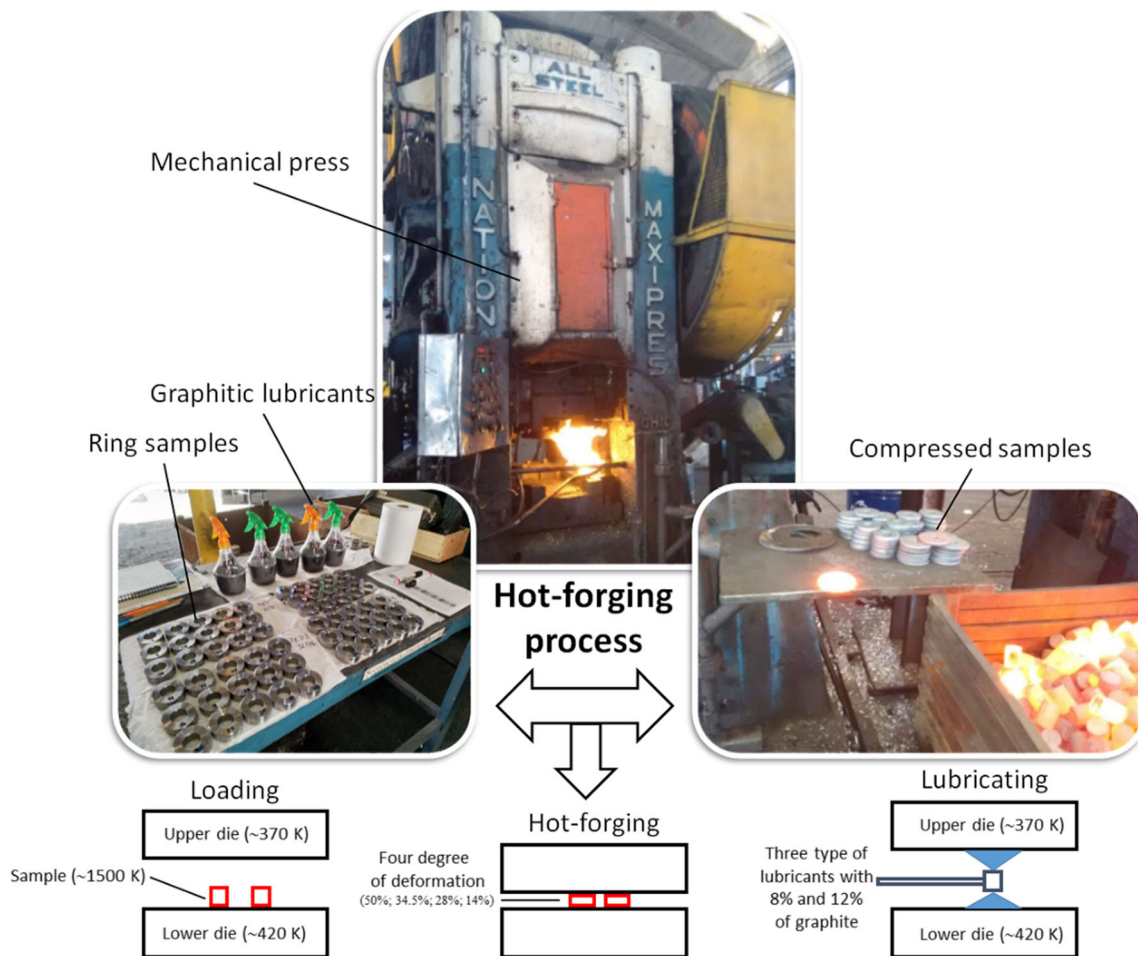


Fig. 2 Schematic of the mechanical press equipped with the induction furnace used for the ring tests at hot-forging temperatures

concentrations. Horizontal lines of the box plots represent the median and first and third quartile, squares represent the average, whiskers represent the tenth and ninetieth percentile, and crosses below and above the boxplots represent maximum and minimum sided values.

The results show that the lubricant A with 8% of graphite concentration presents the highest average friction coefficient value of 0.47, whereas the lubricant B with 8% of graphite concentration shows the lowest average friction coefficient value of 0.40. Additionally, no clear differences in the average friction coefficients are found amongst the three lubricants with a 12% of graphite concentration. However, lower dispersion is found while using lubricant B and higher dispersion for lubricant C. According to these results, the lubricant B exhibits lower average friction coefficient values which ensure a lower wear between elements in contact at room temperature. Regarding the friction coefficient differences found amongst the lubricants with different graphite concentrations, it is noted that a greater density of solid suspensions (graphite) tends to increase the friction coefficient, at least for the lubricants B and C.

3.3 Tribology behavior for temperatures over 1400 K

The properties of the lubricant at extreme temperatures are difficult to control, due to the fast matrix evaporation of the lubricant. At these high temperatures, the lubricant distribution on the selected surface is crucial to reduce the friction coefficient values at the interfaces [26], which directly affect the forging load and energy. Subsequently, the ring test is performed to determine the bulk forming of the specimen and the friction coefficient under hot-forging temperatures. To achieve that, a mechanical press equipped with an induction furnace and a lubrication system is used to perform the ring test at temperatures over 1400 K, as described in Fig. 2. Table 4 shows the temperature of the material during compression, the preheating temperature of the upper and lower dies, and radius and height differences of the specimen at the end of the stroke, which are associated with the degree of deformation under compression.

Then, the tribological behavior of the lubricant varies depending on the percentage of bulk compression. Accordingly, Fig. 6 exhibits the relationship between the height and radius differences after the forging process, which shows the bulk

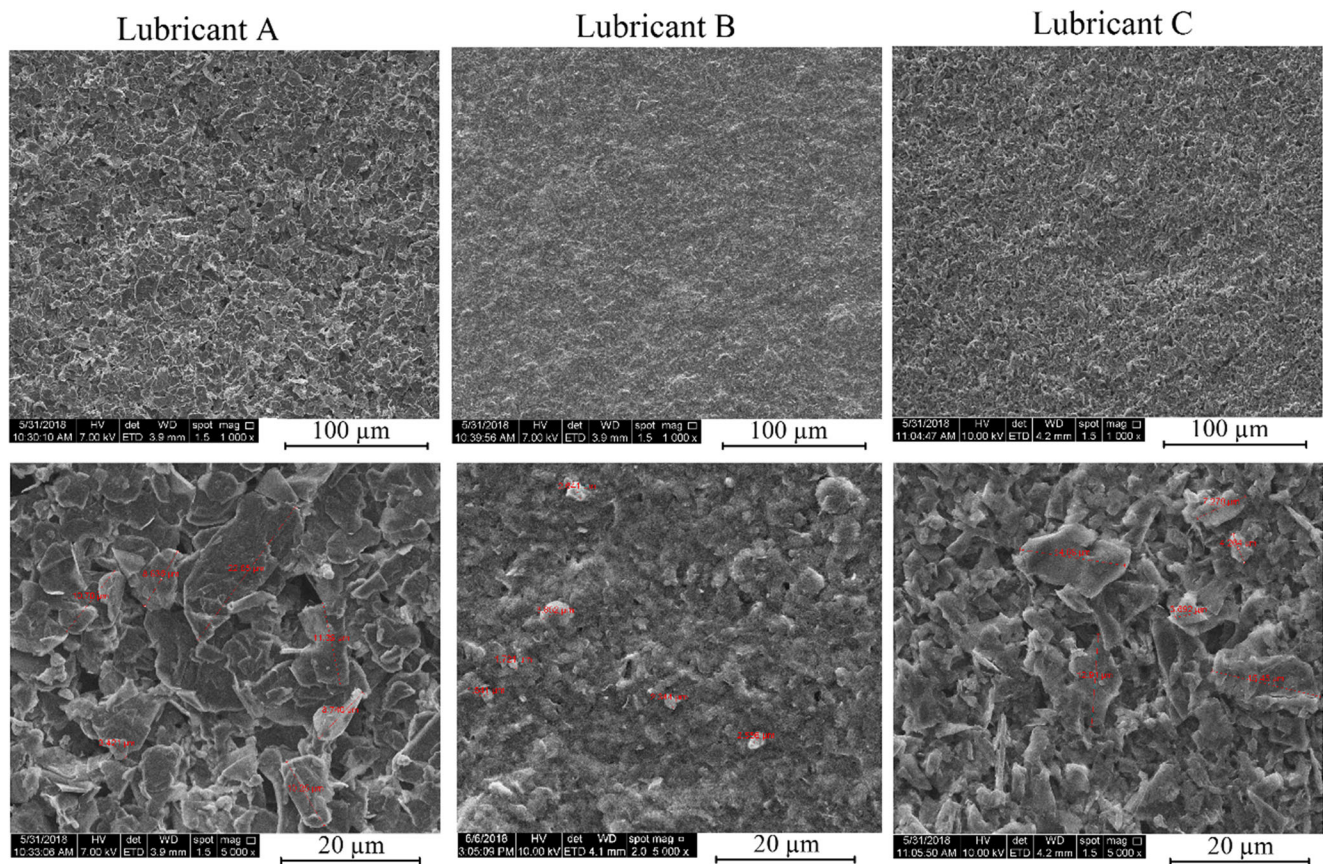


Fig. 3 Matrix distribution and size measurements of the graphite embedded in the matrix for used lubricants as-received from the supplier without diluting

deformation by using three types of lubricants (A, B, and C) and two graphite concentrations (8% and 12%).

The behavior of the lubricants with 8% of graphite concentration presents tribological differences when the degree of bulk deformation reaches 50%; the friction coefficient values are more significant for the lubricants A and C as compared to those for B. Looking at the curve for lubricants with 12% of graphite concentration, the smaller tribological differences are found between the lubricants even for low degree of deformation. In particular, the lubricant B with 12% of graphite concentration exhibits the lowest friction for the highest degree of deformation. Therefore, the lubricants become more effective when greater graphite concentrations are

combined with higher degree of deformation at hot-forging temperatures. Consequently, the solid suspension becomes crucial to improve the friction coefficient, since the lubricant's matrix quickly evaporates at extreme temperatures [21, 22]. Figure 7 describes the tribological behavior of the same type of lubricants for different graphite concentrations to emphasize the characterization of the lubricants. Subsequently, the effectiveness of using higher percentage of graphite (solid suspensions) in the three lubricants can be analyzed.

Regarding the graphite concentration for each type of lubricant, greater axial and radial deformations are found, when a larger degree of compression deformation is assessed. Additionally, smaller deformations are observed when higher

Table 3 Percent of the chemical elements and the average size of the graphite embedded

Type of lubricant	Chemical composition (%wt)					Av. graphite size (μm)
	C	O	Na	Al	Si	
Lub A	79.06	16.01	2.45	0.1	2.38	10.86 ± 5.45
Lub B	78.41	13.97	2.08	0.29	4.95	2.41 ± 0.67
Lub C	81.44	12.98	1.17	0.2	3.89	9.85 ± 4.72

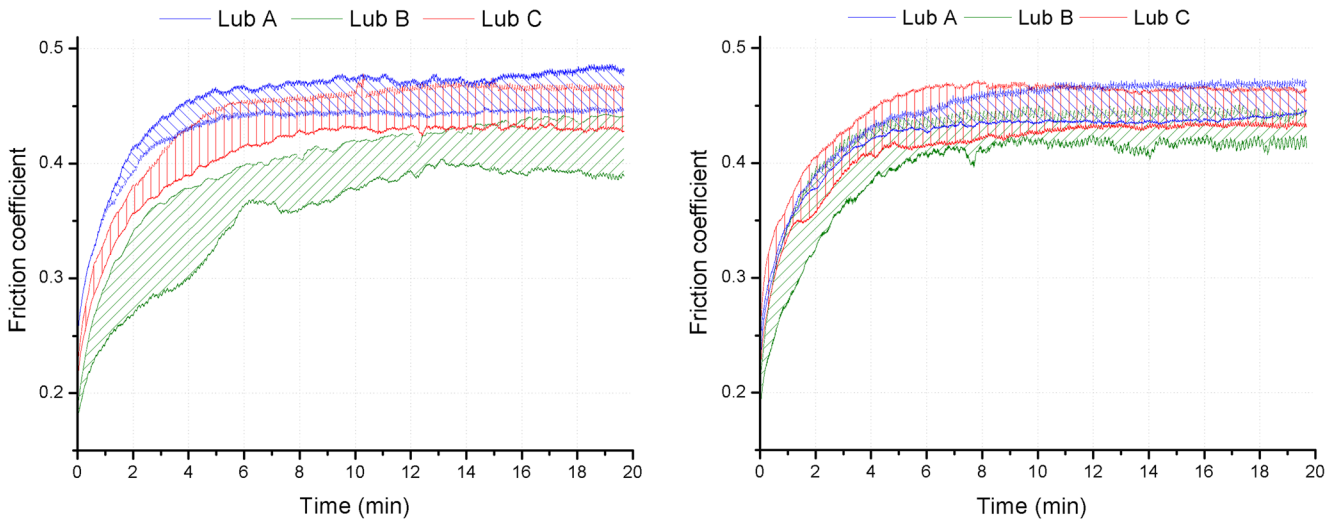


Fig. 4 Time-dependent friction curves for the three types of lubricants and concentration of graphite of 8% (left side) and 12% (right side)

percentage of graphite is embedded in the lubricant's matrix, independently of the lubricant type. Lubricants A and B exhibit a higher dispersion in the tribological behavior between the two graphite concentrations, what tend to remain constant for medium and high degree of deformations. In particular, for bulk deformations of 30% are found the biggest tribological difference between the two concentrations, 35% for lubricant A and 19% for lubricant B. On the other side, lubricant C does not show significant tribology differences between the graphite concentrations and the bulk forming configurations. Then, the friction coefficient for each configuration is studied from the relationship of the percentage of reduction of the height and the internal diameter of the specimen after hot-forging test. Accordingly, the friction

coefficient can be calculated by using the well-known Male and Cocroft [27] equation:

$$\mu = \frac{1}{\sqrt{3}} \left(\frac{-1}{2 \frac{R_0}{h} \left(1 + \frac{R_i}{R_0} - 2 \frac{R_n}{R_0} \right)} \right) \cdot \ln \left[\left(\frac{R_i}{R_0} \right)^2 \cdot \frac{\left(\frac{R_n}{R_0} \right)^2 + \sqrt{3 + \left(\frac{R_n}{R_0} \right)^4}}{\left(\frac{R_n}{R_0} \right)^2 + \sqrt{3 \left(\frac{R_i}{R_0} \right)^4 + \left(\frac{R_n}{R_0} \right)^2}} \right] \quad (1)$$

$$R_n = R_{\text{ext}} \sqrt{\frac{\left(\frac{R_i}{R_0} \right) + \left(\frac{\Delta R_i}{\Delta R_0} \right)}{\left(\frac{R_0}{R_i} \right) + \left(\frac{\Delta R_i}{\Delta R_0} \right)}} \quad (2)$$

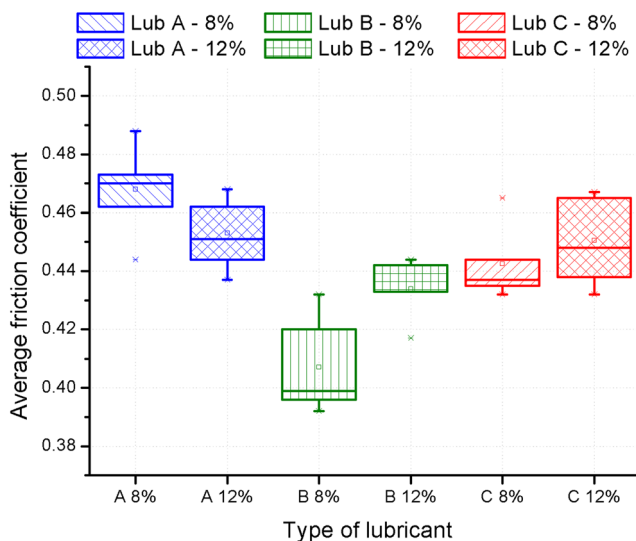


Fig. 5 Boxplot of the friction coefficient at the stable zone of friction curve for the three types of lubricants and concentration of graphite of 8% and 12%

where R_n is the average radius of sample, R_i is the inner radius after deformation, R_0 is the external radius after deformation, ΔR_i is the difference of the internal radius during the process, ΔR_0 is the difference of external radius during the process, h is the height of the sample, and μ is the friction coefficient. Therefore, the estimated friction coefficient of each configuration is listed in Table 5.

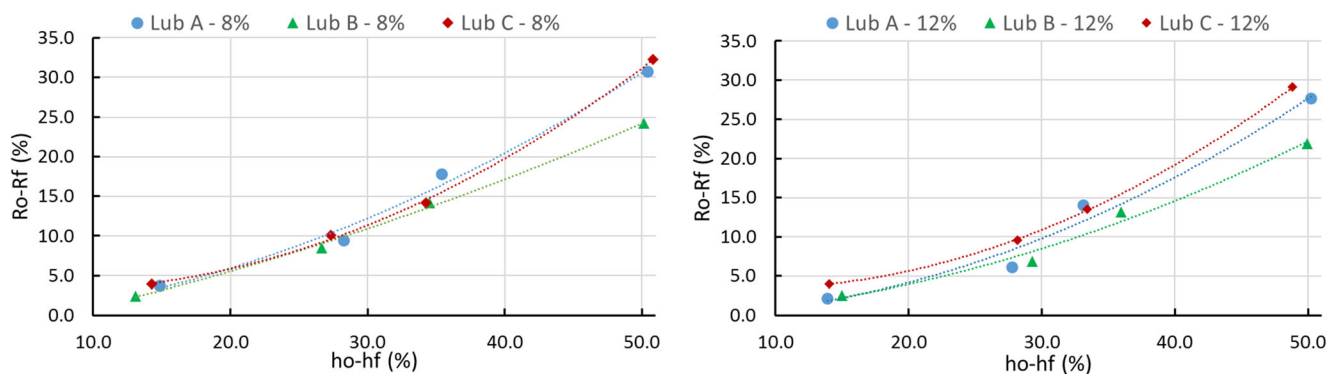
The friction coefficients obtained from the Male and Cocroft equation denote a decrease of the values when a larger degree of deformation is applied. In particular, when the bulk deformation increases, the friction coefficient decreases and the lubricant effectiveness increases. Besides, lower friction values are found when higher concentration of graphite is embedded in the lubricant matrix. However, lubricant C does not follow the same trend, since the percentage of graphite seems to not have an influence on reducing the friction coefficient. Figure 8 denotes the theoretical friction coefficients for each configuration calculated with the Male-Cocroft Eq. (1).

Table 4 Measurements of temperature and height and radius difference during the ring test at the hot-forging temperature for the three lubricants and two graphite concentrations

Lubricant type	Graphite (%)	T ^a (K)	T ^a lower die (K)	T ^a upper die (K)	R ₀ -R _f (%)	h ₀ -h _f (%)
A	8	1501	433	378	3.7	14.8
		1506	423	368	9.5	28.2
		1497	428	368	17.9	35.4
		1485	408	358	30.8	50.4
	12	1503	438	363	2.2	13.9
		1453	423	363	6.1	27.8
		1497	438	383	14.0	33.1
		1509	453	353	27.6	50.2
B	8	1473	433	378	2.4	13.1
		1523	418	373	8.5	26.7
		1473	448	368	14.1	34.5
		1519	418	363	24.2	50.2
	12	1487	433	373	2.5	15.0
		1483	423	373	6.9	29.3
		1499	400	358	13.2	36.0
		1473	438	373	21.9	49.9
C	8	1510	418	368	3.9	14.3
		1493	423	363	10.1	27.3
		1503	418	363	14.2	34.3
		1523	408	358	32.3	50.8
	12	1509	438	368	4.0	14.0
		1493	418	368	9.6	28.2
		1483	418	378	13.5	33.4
		1489	448	363	29.1	48.8

First of all, a greater degree of deformation in the hot-forging process seems to decrease the friction coefficient, independently of the lubricant type and graphite concentration. Furthermore, lower values of the friction coefficients are denoted when higher concentrations of graphite are used, as it is observed in lubricants A and B. The decrease of friction coefficient is emphasized when the largest degree of bulk deformation (50%) is applied. In particular, lubricant B with 12% of graphite concentration shows the lowest friction value of 0.21.

The greatest friction coefficient is found when low bulk deformations are used combined with the lubricant C and 12% of graphite concentration. In this case, the friction coefficient increases up to 0.41. Therefore, lubricants embedded with finer particles and combined with higher density of some chemical elements, that increase the chances of formation of silicate compounds and alumina (Na_2SiO_3 , SiO_2 , and Al_2O_3 amongst others), seem to have an influence on reducing the friction coefficient, while the percentage of graphite

**Fig. 6** Tribology behavior over the degree of bulk deformation for the three types of lubricants with two concentrations of graphite: 8% (left side) and 12% (right side)

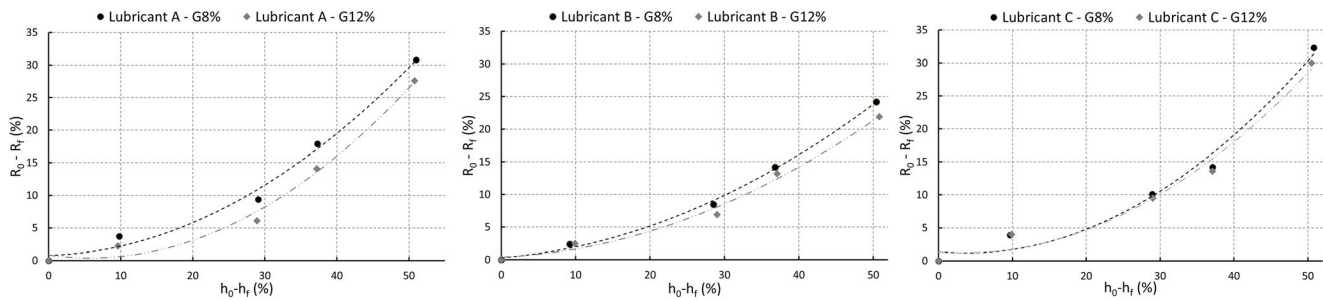


Fig. 7 Tribology behavior of the three types of lubricants, i.e., A, B, and C, and the two concentrations of graphite, i.e., 8% and 12%

concentration can noticeably reduce the friction coefficient when larger deformations are assessed during hot-forging temperatures. Accordingly, Gunda and Narala [24] described the enhancement of the tribology capabilities when smaller size of particles is embedded in the matrix, due to it is favored the formation of a continuous and effective film thickness at the interfaces. Finally, Bratz [28] stated that finer particles facilitate a better surface distribution of the lubricant which helps to reduce the wear of the interacting surfaces by

promoting sliding mechanisms and, consequently, ensure a longer lifespan of those surfaces.

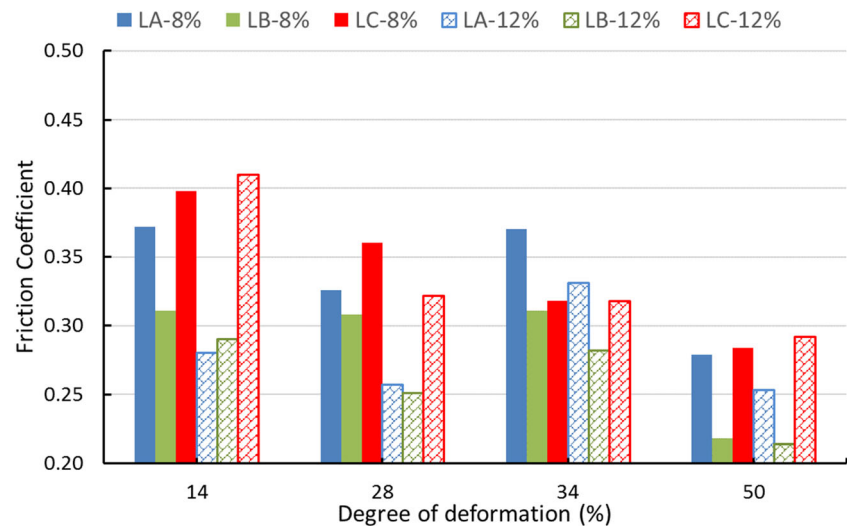
4 Conclusions

The present paper evaluates the friction capabilities of three different graphitic lubricants with two graphite concentrations

Table 5 Friction coefficients for each type of lubricant and graphite concentration during a ring test under hot-forging temperatures

Lubricant	Graphite (%)	Degree of deformation (%)	Geometrical measurements			R_n (mm)	μ
			D_i (mm)	D_0 (mm)	h (mm)		
A	8	14.81	26.54	58.10	15.59	16.29	0.372
		28.24	24.97	61.99	13.16	16.22	0.326
		35.37	22.56	64.83	11.86	16.26	0.370
		50.38	19.01	71.45	9.11	15.34	0.279
	12	13.92	26.95	58.39	15.71	15.28	0.280
		27.76	25.34	62.31	13.22	15.15	0.257
		33.08	23.68	64.30	12.26	16.12	0.331
		50.22	19.94	71.66	9.11	15.29	0.253
B	8	13.09	26.87	57.81	15.80	15.71	0.311
		26.66	25.17	62.36	13.34	15.86	0.308
		34.52	23.49	64.71	11.91	15.92	0.311
		50.17	20.85	72.02	9.05	15.05	0.218
	12	15.02	26.88	58.35	15.56	15.49	0.290
		29.27	25.70	62.91	12.95	15.47	0.251
		35.96	23.93	65.18	11.70	15.82	0.282
		49.92	21.52	71.93	9.16	15.17	0.214
C	8	14.29	26.48	58.01	15.66	16.39	0.398
		27.34	24.77	61.94	13.29	16.32	0.360
		34.28	23.69	64.65	12.02	16.06	0.318
		50.82	18.67	71.62	9.00	15.30	0.284
	12	14.04	26.48	58.11	15.73	16.47	0.410
		28.17	24.94	62.23	13.16	16.13	0.322
		33.42	23.84	64.53	12.17	16.00	0.318
		48.85	19.25	70.50	9.31	15.46	0.292

Fig. 8 Estimated friction coefficients over the degree of deformation for different types of lubricants and graphite concentrations



at room and hot-forging temperatures. To this end, the following aspects can be withdrawn:

- The main differences found between the three types of lubricants are attributed to the percentage weight of aluminum and silicon, which can help to reduce the friction coefficient due to the formation of silicate compounds and alumina at the interfaces. Additionally, the size of the graphite particle is another key parameter that can enhance the friction capability of the lubricant under extreme temperatures.
- At room temperature, the lubricant B with 8% of graphite concentration exhibits the lowest friction coefficient, 0.40 in average, while lubricant A with 8% of graphite concentration shows the greatest friction coefficient, 0.47 in average. The lubricants with 12% of graphite concentration do not show any obvious trend on reducing the friction coefficient at room temperature.
- At hot-forging temperatures, the friction coefficients noticeably decrease, independently of the lubricant type and graphite concentration, when larger degrees of deformations are applied. Furthermore, lubricant B with higher graphite concentration exhibits the lowest friction coefficient when the largest bulk deformation is used. In general, higher graphite concentration and larger bulk deformation reduce the friction coefficient, at least for lubricants A and B. Lubricant C does not show an obvious trend.

In future work, it will be analyzed different types of coatings and surface textures in the hot-forging tools with the purpose to reduce friction coefficient and enhance the lifespan of the dies under extreme temperatures. The surface degradation will be also addressed to describe the interaction of the coated surface and different sizes of graphite embedded in the lubricant's matrix.

Acknowledgments CRAFTSA S.A. is acknowledged for their support and contribution to this work. We give thanks to Soledad Pereda from INTI-Mecánica for the valuable support with the electronic microscopy and X-ray spectroscopy analysis.

Funding information This work is supported by the Ministry of Economy and Competitiveness of Spain (reference project: FJCI-2016-29297), the National Council for Scientific and Technological Development of Chile (Fondecyt project 3180006), and the Aeronautics Advanced Manufacturing Center (CAFA) of Bilbao.

Compliance with ethical standards

Conflict of interest The authors declare that they have no conflict of interest.

Publisher's note Springer Nature remains neutral with regard to jurisdictional claims in published maps and institutional affiliations.

References

1. Altan T, Ngaile G, Shen G (2004) Cold and hot forging: fundamentals and applications. ASM International, ISBN: 978-0-87170-805-2
2. Sofuoglu H, Gedikli H, Rasty J (2000) Determination of friction coefficient by employing the ring compression test. J Eng Mater Technol 123(3):338–348. <https://doi.org/10.1115/1.1369601>
3. Camacho AM, Torralvo AI, Bernal C, Sevilla L (2013) Investigations on friction factors in metal forming of industrial alloys. Procedia Eng 63:564–572. <https://doi.org/10.1016/j.proeng.2013.08.240>
4. González HA, Sánchez Egea AJ, Travieso-Rodríguez JA, Llumà i Fuentes J, Jorba Peiró J (2018) Estimation of the polishing time for different metallic alloys in surface texture removal. Mach Sci Technol 22:1–13. <https://doi.org/10.1080/10910344.2017.1402931>
5. Valero J, Marín MM, Camacho AM (2015) Influence of load application methodology in the performance of ring compression tests. Procedia Eng 132:306–312. <https://doi.org/10.1016/j.proeng.2015.12.499>
6. Camacho AM, Veganzones M, Claver J, Martín F, Sevilla L, Ángel Sebastián M (2016) Determination of actual friction factors in metal

- forming under heavy loaded regimes combining experimental and numerical analysis. *Materials* 9(9), 751:1–9. <https://doi.org/10.3390/ma9090751>
7. Kim H, Altan T (2010) Tribology in forming advanced high strength steels: evaluation of lubricants, tool materials and coatings for reducing galling. LAP Lambert academic publishing, Saarbrücken ISBN: 978-3-8383-0590-5
8. Oliveira RA, Alguero Koller L, Schaeffer L (2003) Evaluation of two commercially-available lubricants by means of ring test to AA 6061 F aluminum alloys. *Mater Res* 6(4):591–597. <https://doi.org/10.1590/S1516-14392003000400028>
9. Mirahmadi SJ, Hamed M, Cheraghzadeh M (2015) Investigating friction factor in forging of Ti-6Al-4V through isothermal ring compression test. *Tribol Trans* 0:1–7. <https://doi.org/10.1080/10402004.2015.1019598>
10. Ohdar RK, Talukdar P, Israr Equbal M (2015) Evaluation of friction coefficient of 38MnVS6 medium carbon micro-alloyed steel in hot forging process by using ring compression test. *Technology Letters* 2(3):12–16 ISSN: 2348–8131
11. Shahriari D, Amiri A, Sadeghi MH (2010) Study on hot ring compression test of Nimonic 115 superalloy using experimental observations and 3D FEM simulation. *JMEPEG* 19:633–642. <https://doi.org/10.1007/s11665-009-9522-7>
12. Hu C, Ou H, Zhao Z (2015) An alternative evaluation method for friction condition in cold forging by ring with boss compression test. *J Mater Process Technol* 224:18–25. <https://doi.org/10.1016/j.jmatprotec.2015.04.010>
13. Hu C, Yin Q, Zhao Z, Ou H (2017) A new measuring method for friction factor by using ring with inner boss compression test. *Int J Mech Sci* 123:133–140. <https://doi.org/10.1016/j.ijmecsci.2017.01.042>
14. Sánchez Egea AJ, Deferrari N, Abate G, Martínez Krahmer D, López de Lacalle LN (2018) Short-cut method to assess a gross available energy in a medium-load screw friction press. *Metals* 8(3), 173:1–12. <https://doi.org/10.3390/met8030173>
15. Cristino VAM, Rosa PAR, Martins PAF (2015) The role of interfaces in the evaluation of friction by ring compression testing. *Exp Tech* 39:47–56. <https://doi.org/10.1111/j.1747-1567.2012.00857.x>
16. Cristino VAM, Rosa PAR, Martins PAF (2011) Surface roughness and material strength of tribo-pairs in ring compression tests. *Tribol Int* 44:134–143. <https://doi.org/10.1016/j.triboint.2010.10.002>
17. Matsumoto R, Harada S, Utsunomiya H (2015) Influence of oxide scale formed on chrome steel surface in steam atmosphere on deformation behavior of chrome steel in hot ring compression. *ISIJ Int* 55(8):1711–1720. <https://doi.org/10.2355/isijinternational.ISIJINT-2014-754>
18. Zhu Y, Zeng W, Ma X, Tai Q, Li Z, Li X (2011) Determination of the friction factor of Ti-6Al-4V titanium alloy in hot forging by means of ring-compression test using FEM. *Tribol Int* 44:2074–2080. <https://doi.org/10.1016/j.triboint.2011.07.001>
19. Dohda K, Boher C, Rezai-Aria F, Mahayotsanun N (2015) Tribology in metal forming at elevated temperatures. *Friction* 3(1):1–27. <https://doi.org/10.1007/s40544-015-0077-3>
20. Li LX, Peng DS, Liu JA, Liu ZQ (2001) An experiment study of the lubrication behavior of graphite in hot compression tests of Ti-6Al-4V alloy. *J Mater Process Tech* 112(1):1–5. [https://doi.org/10.1016/S0924-0136\(00\)00845-1](https://doi.org/10.1016/S0924-0136(00)00845-1)
21. Asai K, Kitamura K (2014) Estimation of frictional property of lubricants for hot forging of steel using low-speed ring compression test. *Procedia Engineering* 81:1970–1975. <https://doi.org/10.1016/j.proeng.2014.10.266>
22. Asai K, Kitamura K, Yukawa N, Hayashi N (2017) Estimation of friction by using improved calibration curves of ring compression test for hot forging of steel. *Procedia Engineering* 207:2280–2285. <https://doi.org/10.1016/j.proeng.2017.10.995>
23. Sánchez Egea AJ, Martynenko V, Martínez Krahmer D, López de Lacalle LN, Benítez A, Genovese G (2018) On the cutting performance of segmented diamond blades when dry-cutting concrete. *Materials* 11:1–12. <https://doi.org/10.3390/ma11020264>
24. Gunda RK, Narala SKR (2016) Tribological studies to analyze the effect of solid lubricant particle size on friction and wear behaviour of Ti-6Al-4V alloy. *Surf Coat Technol* 308:203–212. <https://doi.org/10.1016/j.surfcoat.2016.06.092>
25. Devendra Singh GD, Sivakumar Konathala LN, Prasad VVDN (2016) Friction reduction capabilities of silicate compounds used in an engine lubricant on worn surfaces. *Adv Tribol* 1901493:1–10. <https://doi.org/10.1155/2016/1901493>
26. Yang L, Shivpuri R (2007) An isothermal finite difference model for droplet spread in the spraying of hot die surfaces with water-based graphite lubricants. *J Manuf Sci Eng* 129(5):874–884. <https://doi.org/10.1115/1.2752525>
27. Male AT, Cocroft MG (1964) A method for the determination of the coefficient of friction of metals under condition of bulk plastic deformation. *J Inst Metals* 93:38–46
28. Bartz WJ (1972) Some investigations on the influence of particle size on the lubricating effectiveness of molybdenum disulfide. *ASLE Trans* 15(3):207–215. <https://doi.org/10.1080/05698197208981418>